Novel multi-spin-state linear hexanickel complexes Ni_6^{11+} and their singly oxidized products Ni_6^{12+} with 1,8-naphthyridine-based ligands: Tuning the redox properties of the metal string

Ting-Bin Tsao [a], Shang-Shih Lo [b], Chen-Yu Yeh [b,*], Gene-Hsiang Lee [a], Shie-Ming Peng [a,c,*]

[a] *Department of Chemistry, National Taiwan University, No. 1, Sec. 4, Roosevelt Road, Taipei 106, Taiwan*
[b] *Department of Chemistry, National Chung Hsing University, Taichung 402, Taiwan*
[c] *Institute of Chemistry, Academia Sinica, Taipei 115, Taiwan*

Abstract

The new ligand, 2,7-bis(α-pyrimidylamino)-1,8-naphthyridine (H_2bpmany), was prepared by the reaction of 2,7-dichloro-1,8-naphthyridine with 2-aminopyrimidine in the presence of sodium *tert*-butoxide under palladium-catalyzed conditions. The linear hexanickel Ni_6^{11+} complexes $[Ni_6(\mu_6$-bpmany$)_4X_2]Cl$ (X = Cl (**1**); X = NCS (**2**)) and their singly oxidized products $[Ni_6(\mu_6$-bpmany$)_4X_2](BF_4)_2$ (X = Cl (**3**); X = NCS (**4**)) have been synthesized, and compounds **1**, **2** and **4** have been crystallographically characterized. The crystal structures of the Ni_6^{11+} complexes show remarkably short Ni–Ni distances (ca. 2.22 Å), clearly indicative of partial metal–metal bonding in the mixed-valence Ni_2^{3+} unit. This is also verified by the axial X-band EPR spectra of the complexes in solution. Magnetic susceptibility measurements reveal that the Ni_6^{11+} complexes exhibit antiferromagnetic interactions ($J = -47$ cm^{-1}) between the terminal Ni^{2+} ion and the central Ni_2^{3+} unit, and the Ni_6^{12+} complexes exhibit weak antiferromagnetic interactions ($J = -5$ cm^{-1}) between the two terminal Ni^{2+} ions. The cyclic voltammograms display three reversible redox waves at $E_{1/2}^{(1)} = +0.87$, $E_{1/2}^{(2)} = -0.02$ and $E_{1/2}^{(3)} = -0.46$ V for **1**, and $E_{1/2}^{(1)} = +0.96$, $E_{1/2}^{(2)} = -0.01$, and $E_{1/2}^{(3)} = -0.41$ V for **2**. The relatively low potentials of $E_{1/2}^{(2)}$ suggest that the Ni_6^{11+} complexes can be easily converted to their Ni_6^{12+} forms.
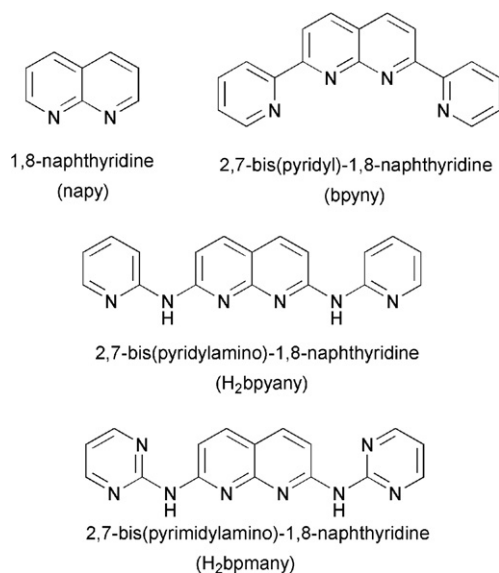© 2007 Elsevier Ltd. All rights reserved.

1. Introduction

Linear multinuclear metal complexes continue to attract much attention from inorganic chemists because of their fascinating chemistry such as spin interactions, metal–metal bonding and their potential application in molecular metal wires, since the first reports of trinuclear copper and nickel complexes wrapped by four di-α-pyridylamido ligands in 1990–1991 [1,2]. In the past decade, a number of tri- [3–7], tetra- [8], penta- [9–11], hepta- [8,12,13], and nonanuclear [14] metal string complexes with oligo-(α-pyridyl)amido

ligands have been synthesized and structurally characterized. While extensive studies have been carried out on the metal string complexes with odd numbers of metal atoms, studies on the counterparts with even numbers of metal atoms are relatively rare. Recently, we have successfully synthesized a series of 1,8-naphthyridine-modified ligands and their corresponding multinuclear metal complexes. The 1,8-naphthyridine-based ligands are attractive candidates for building linear metal string complexes because the 1,8-naphthyridyl unit is rigid and potentially redox active. Scheme 1 shows the structures of some 1,8-naphthyridine-modified ligands. The preparation and properties of the corresponding complexes of these ligands have been reported [15–17]. In particular a series of mixed-valence compounds $[Ni_2(napy)_4X_2](BPh_4)$ (X = Cl, Br, I) has been

---

* Corresponding authors. Tel.: +886 2 23638305; fax: +886 2 83693765.
E-mail addresses: cyyeh@dragon.nchu.edu.tw (C.-Y. Yeh), smpeng@ntu.edu.tw (S.-M. Peng).

Scheme 1. Structure of 1,8-naphthyridine and its derivatives.

isolated in which each nickel ion has a formal charge of +1.5. The magnetic properties of $[Ni_2(napy)_4Br_2]^+$ reveal that the ground spin-state of the system is in a quartet state. Recently, we have reported the synthesis and structural studies of linear hexa-cobalt and -nickel complexes, in which the metal chain is supported by four 1,8-naphthyridine-based bpyany^{2-} ligands (Scheme 1) [18,19]. On the basis of the X-ray structure analysis, the $Co_6^{11+/12+}$ complexes have delocalized electronic structures whereas the $Ni_6^{11+/12+}$ complexes can be regarded as localized ones.

Here we describe the synthesis, crystal structures, and electrochemical and magnetic properties of novel linear hexanickel string complexes $[Ni_6(\mu_6\text{-bpmany})_4X_2]Cl$ (X = Cl (1); X = NCS (2)), and their singly oxidized products $[Ni_6(\mu_6\text{-bpmany})_4X_2](BF_4)_2$ (X = Cl (3); X = NCS

(4)), where bpmany is the dianion of 2,7-bis(α-pyrimidyl-amino)-1,8-naphthyridine.

2. Results and discussion

2.1. Synthesis

The new ligand, 2,7-bis(α-pyrimidylamino)-1,8-naph-thyridine (H$_2$bpmany), was prepared in good yield by pal-ladium-catalyzed cross-coupling of 2-aminopyrimidine with 2,7-dichloro-1,8-naphthyridine, and characterized by ^{1}H NMR and FAB mass spectrometry. The reaction of H$_2$bpmany with Ni(OAc)$_2 \cdot$ 4H$_2$O in a 4:6 ratio in refluxing naphthalene, followed by addition of excess LiCl or NaSCN generates $[Ni_6(\mu_6\text{-bpmany})_4X_2]Cl$ (X = Cl (1); X = NCS (2)). The presence of the Cl$^-$ counter anion in 2 may be explained by the presence of a small amount of Cl$^-$ anion produced by dissociation of CH$_2$Cl$_2$ [20], which is the only source of chloride ion in the synthesis of this compound. In this reaction, the desired product was expected to be a hexanickel complex with six Ni^{2+} ions. However, the reaction gave a mixed valence species that has five Ni^{2+} ions and one Ni$^+$ ion. Based on the electro-chemical data, as will be discussed later on, one of the redox potentials was observed at about 0.00 V vs. Ag/AgCl. This indicates that the form $[Ni_6(\mu_6\text{-bpmany})_4X_2]^{2+}$ is relatively easy to reduce to $[Ni_6(\mu_6\text{-bpmany})_4X_2]^+$. Under the reaction conditions, any reagents in an excess amount or even the solvent could be the source of reducing agent. Treatment of 1 or 2 with $[Cp_2Fe]BF_4$ in CH$_2$Cl$_2$ gives dark brown crystals of the singly oxidized complexes $[Ni_6\text{-}(\mu_6\text{-bpmany})_4X_2](BF_4)_2$ (X = Cl (3); X = NCS (4)). It should be mentioned that complexes 1–4 can be prepared under air, and are found to be air-stable in the solid state. The IR active C≡N stretching vibration was observed at 2067 cm^{-1} for both 2 and 4.

Table 1
Crystallographic data for complexes 1, 2 and 4

	$1 \cdot 4.5CH_2Cl_2 \cdot 0.5H_2O$	$2 \cdot 5CH_2Cl_2 \cdot 0.5CH_3CN$	$4 \cdot 2CH_3CN \cdot 2Et_2O$
Formula	$C_{68.5}H_{50}N_{32}Cl_{12}Ni_6O_{0.5}$	$C_{72}H_{51.5}Cl_{11}N_{34.5}Ni_6S_2$	$C_{78}H_{66}B_2F_8N_{36}Ni_6O_2S_2$
Formula weight	2107.06	2206.31	2129.67
Crystal size (mm)	$0.50 \times 0.18 \times 0.03$	$0.50 \times 0.15 \times 0.10$	$0.37 \times 0.10 \times 0.10$
Crystal system	monoclinic	tetragonal	monoclinic
Space group	$C2/c$	$P4/n$	$P2_1/c$
a (Å)	31.0776(10)	28.7185(5)	11.1541(1)
b (Å)	16.1371(5)	28.7185(5)	16.7568(2)
c (Å)	34.2316(11)	11.0775(2)	23.2990(3)
β (°)	105.2450(12)		91.0548(7)
V (Å^3)	16563.1(9)	9136.2(3)	4354.01(9)
Z	8	4	2
ρ (Mg m^{-3})	1.690	1.604	1.624
θ Range for collection (°)	1.23–25.00	1.42–25.00	1.50–27.50
Absorption coefficient (mm^{-1})	1.788	1.641	1.406
Maximum, minimum transmission	0.934, 0.674	0.869, 0.666	0.875, 0.736
Measured reflections	67,846	43,566	50,910
Unique reflections [R_{int}]	14,500 [0.0790]	8026 [0.0677]	9996 [0.0585]
R_1, wR_2 $(I > 2\sigma(I))$[a]	0.1156, 0.3488	0.1085, 0.3117	0.0765, 0.2366
R_1, wR_2 (all data)[a]	0.1824, 0.3940	0.1625, 0.3575	0.1258, 0.2722

[a] $R_1 = \sum|F_o - F_c|/\sum|F_o|$; $wR_2 = [\sum w|F_o^2 - F_c^2|^2/\sum wF_o^4]^{1/2}$.

2.2. Structures

Complex **1** crystallizes in space group $C2/c$ and the structure consists of the hexanickel cation [Ni$_6$(bpmany)$_4$-Cl$_2$]$^+$ and a Cl$^-$ anion. Complex **2** crystallizes in space group $P4/n$ and the cation resides on an inversion center with 50% disorder of a spiral set of four bpmany^{2-} ligands. The [Ni$_6$(μ_6-bpmany)$_4$]$^{3+}$ cation in both complexes **1** and **2** is roughly in a D_4 symmetry and the linear Ni$_6$ unit is supported by four bpmany^{2-} ligands in a spiral configuration (Figs. 1 and 2). Thus, the average bond lengths for complexes **1** and **2** were calculated by a D_4 symmetry (Table 2). In the hexanickel chain of compounds **1** and **2**, the terminal nickel ions (Ni(1) and Ni(6)) are square pyramidal whereas Ni(2)–Ni(5) are square planar. The redox active center should be Ni(3) and Ni(4) which gives a Ni$_2^{3+}$ unit. The average Ni–Ni distances from outer to inner are 2.409(2), 2.289(2) and 2.221(2) Å for **1**, and 2.408(2), 2.304(2) and 2.218(2) Å for **2**. The average Ni–Cl bond distance of 2.307(3) Å in **1** is in the range of Ni–Cl bond lengths for the analogous complexes [Ni$_n$L$_4$Cl$_2$] where L is an oligo-(α-pyridyl)amido ligand. The Ni–N$_{pm}$ distance is 2.08(1) Å, which is longer by about 0.20 Å than Ni–
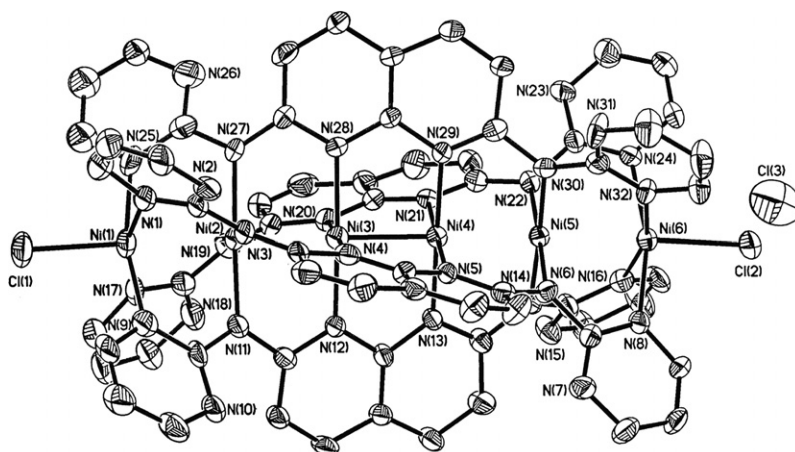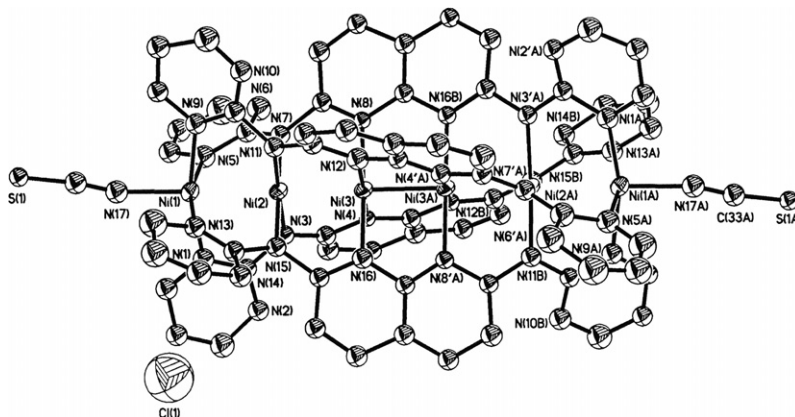
Table 2
Average bond distances (Å) and torsion angles (°) for complexes **1**, **2** and **4**

	1	**2**	**4**
Ni(1)–Ni(2)	2.409(2)	2.408(2)	2.404(1)
Ni(2)–Ni(3)	2.289(2)	2.304(2)	2.306(1)
Ni(3)–Ni(4)	2.221(2)	2.218(2)	2.275(1)
Ni–X	2.307(3)	1.988(9)	2.063(5)
Ni(1)–N$_{pm}$	2.08(1)	2.08(1)	2.08(1)
Ni(2)–N$_{amido}$	1.93(1)	1.92(2)	1.89(1)
Ni(3)–N$_{napy}$	2.01(1)	2.03(2)	1.92(1)
N$_{pm}$–Ni–Ni–N$_{amido}$ torsion	23.96	24.52	22.47
N$_{amido}$–Ni–Ni–N$_{napy}$ torsion	15.19	14.03	16.44
N$_{napy}$–Ni–Ni–N$_{napy}$ torsion	13.79	13.15	15.32

N$_{amido}$ and Ni–N$_{napy}$ distances, suggesting that the terminal Ni^{II} ions are in a high-spin state and the internal ones in a low-spin state.

The singly oxidized complex **4** crystallizes in the monoclinic space group $P2_1/c$ with $Z = 2$. The dication resides on an inversion center with 50% disorder of a spiral set of four bpmany^{2-} ligands, and the positive charges are compensated by two BF$_4^-$ ions (Fig. 3). The Ni–Ni distances of **4** from outer to inner are 2.404(1), 2.306(1) and

Fig. 1. ORTEP drawing of complex **1**. Thermal ellipsoids are drawn at the 30% probability level. Hydrogen atoms are omitted for clarity.

Fig. 2. ORTEP drawing of complex **2**. Thermal ellipsoids are drawn at the 30% probability level. Hydrogen atoms are omitted for clarity.

2.275(1) Å. Removal of one electron from **2** results in an increase in the central Ni–Ni distance from 2.218(2) to 2.275(1) Å and a decrease in the Ni–N_{napy} distance from 2.03(2) to 1.92(1) Å. This indicates that the electron is abstracted from the central Ni_2 unit. In the analoguous complex $[Ni_6(bpyany)_4(NCS)_2](PF_6)$ [19], a similar trend in the structural changes has also been observed when an electron was removed from the Ni_6 chain.

To get further insight on the structures of these complexes, EPR measurements have been performed. The X-band EPR spectra of frozen **1** and **2** are illustrated in Fig. 4, and show signals at $g_\perp = 2.34$ and $g_\parallel = 2.14$ for **1**, and $g_\perp = 2.31$ and $g_\parallel = 2.14$ for **2**, which are consistent with the expected spin-state of $S = 1/2$ in the central Ni_2^{3+} unit. In contrast, no EPR signals were observed for **3** and **4**, consistent with antiferromagnetic coupling of the unpaired electrons in the molecules.

To see if the symmetrical structure of the Ni_6^{11+} complexes persist in solution, the ^1H NMR spectrum of **2** was examined. For a symmetrical molecule, three peaks for the eight equivalent pyrimidyl groups and two peaks for the four equivalent naphthyridyl groups should be observed. As shown in Fig. 5, the spectrum consists of five signals at 72.66, 20.89, 18.81, 15.64 and 12.86 ppm corresponding to the $bpmany^{2-}$ protons, and is consistent with a D_4 symmetry for the $[Ni_6(\mu_6\text{-}bpmany)_4(NCS)_2]^+$ core and paramagnetism of the complex.

As mentioned, the Ni_6^{n+} complexes can be considered as roughly D_4. The central Ni_2N_8 unit is practically half way between the eclipsed and staggered conformations. The mixed-valence $[Ni_2(napy)_4X_2]^+$ (X = halogen) cations have a spin state of $S = 3/2$. In contrast, the dinickel unit of **1** and **2** is in a spin-state of $S = 1/2$. A qualitative MO energy-level diagram for the central $Ni_6^{3+/4+}$ units of our complexes in a square planar coordination environment is shown in Scheme 2. This MO picture can be used to rationalize the observed magnetic properties which correspond to a system with one unpaired electron.
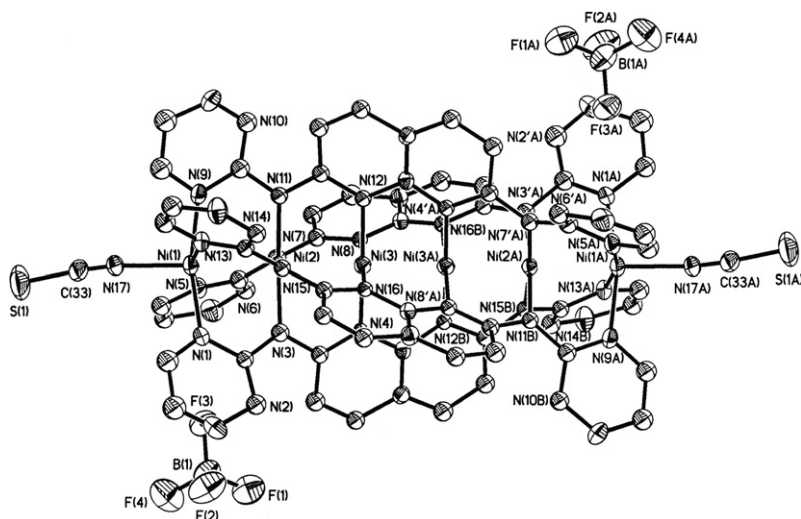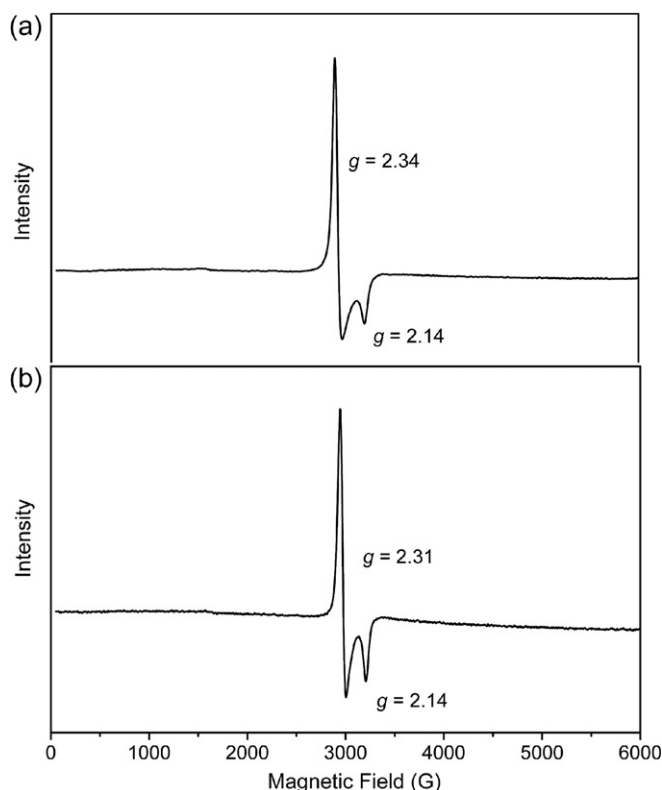

Fig. 4. X-band EPR spectrum of (a) **1** and (b) **2** taken in dichloromethane glass at 77 K.

2.3. Magnetic properties

The magnetic susceptibility of **1–4** were measured in the temperature range of 2–300 K. Compounds **1** and **2** exhibit similar magnetic properties. As an example, Fig. 6 shows the magnetic behavior of **2**. At 300 K the effective magnetic moments of 4.54 and 4.58 μ_B for **1** and **2**, respectively, are close to the spin-only value of 4.36 μ_B expected for a system with three spin states of $S = 1$, $1/2$ and 1. The μ_{eff} values in the range 30–300 K decrease gradually with decreasing

Fig. 3. ORTEP drawing of complex **4**. Thermal ellipsoids are drawn at the 30% probability level. Hydrogen atoms are omitted for clarity.
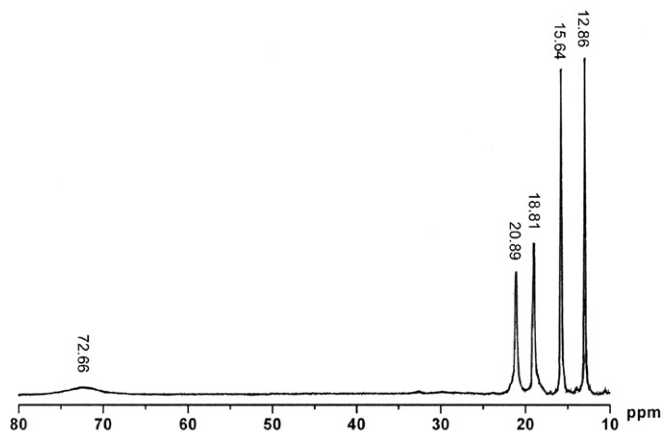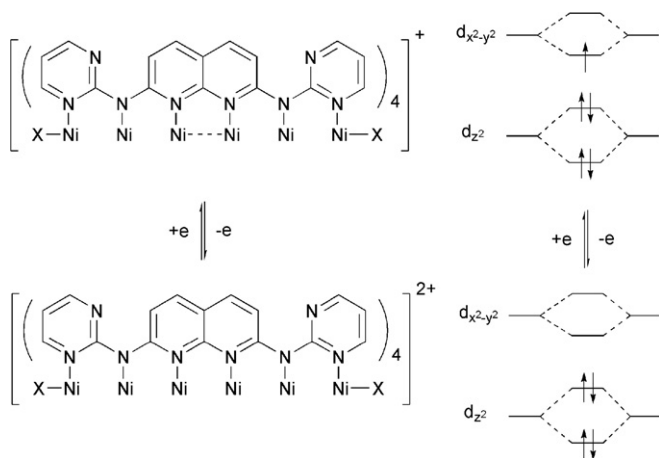
Fig. 5. ^{1}H NMR spectrum of **2** taken at 400 MHz in d_6-DMSO at room temperature.

Scheme 2. The energy level scheme for the central $Ni_2^{3+/4+}$ units in square planar coordination environments in the active electron approximation.
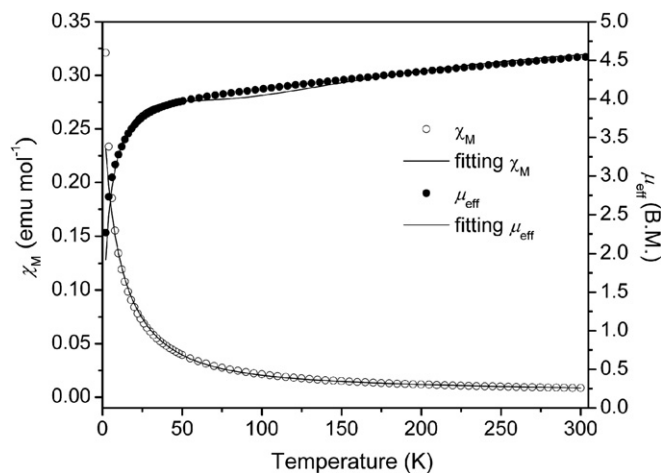

Fig. 6. The magnetic behavior for **2**: molar magnetic susceptibility χ_M (○) and effective magnetic moments μ_{eff} (●). The solid lines are the best-fit curves.

temperature and then decrease sharply to 2.26 and 1.77 μ_B for compounds **1** and **2** at 2 K. These data suggest antiferromagnetic interactions between the terminal Ni^{2+} ion and the central Ni_2^{3+} unit. Taking into account the structural data of this complex, the isotropic spin-exchange for Ni_6^{11+} complex can be given as

$$H = -2J(\widehat{S}_1 \cdot \widehat{S}_{34} + \widehat{S}_6 \cdot \widehat{S}_{34}) - 2J'\widehat{S}_1 \cdot \widehat{S}_6 \quad (1)$$

where J represents the coupling constant to between the terminal Ni^{2+} and central Ni_2^{3+}, and J' is the coupling constant between the two terminal Ni^{2+} ions. Assuming $J' = 0$, the Hamiltonian in Eq. (1) gives rise to five spin states corresponding to the total spin operator $\widehat{S}_T = \widehat{S}_{16} + \widehat{S}_{34}$, i.e., two doublets ($S_T = 1/2$), two quartets ($S_T = 3/2$) and one sextet ($S_T = 5/2$). The molar magnetic susceptibility expression shown in Eq. (2) was then obtained by substituting the energies given in the Heisenberg–Dirac–van Vleck equation [21]

$$\chi_M = \frac{Ng^2\beta^2}{4kT} \times \frac{10 + e^{J/kT} + e^{3J/kT} + 10e^{4J/kT} + 35e^{5J/kT}}{2 + e^{J/kT} + e^{3J/kT} + 2e^{4J/kT} + 3e^{5J/kT}} \quad (2)$$

When impurities are taken into account, χ_M with the Weiss constant is expressed by the following:

$$\chi_M = \frac{Ng^2\beta^2}{4k(T - \theta)} \times \frac{10 + e^{J/kT} + e^{3J/kT} + 10e^{4J/kT} + 35e^{5J/kT}}{2 + e^{J/kT} + e^{3J/kT} + 2e^{4J/kT} + 3e^{5J/kT}}$$
$$\times (1 - \rho) + \frac{2Ng^2\beta^2}{3kT} \times \rho + \chi_{TIP} \quad (3)$$

where N is Avogadro's number, g is the Landé factor, β is the Bohr magneton of the electron, k is the Boltzmann constant, θ is the Weiss constant and T is the temperature in Kelvin. Least-square fitting of the experimental data leads to $J = -46.64$ cm^{-1}, $g = 2.37$, $\theta = -14.28$ K, $\rho = 0$ and TIP $= 0$ with a correlation coefficient of 0.9976 for **1** and $J = -47.27$ cm^{-1}, $g = 2.34$, $\theta = -9.13$ K, $\rho = 0$ and TIP $= 0$ with a correlation coefficient of 0.9976 for **2**. The negative Weiss constants indicate the presence of a dominant antiferromagnetic exchange interaction between the spin carriers. The g values obtained by magnetic measurements are very close to the EPR results of 2.34 for **1** and 2.31 for **2**.

It should be mentioned that under the limiting conditions, Eq. (2) gives a limiting moment of 3.87 BM. Compounds **1** and **2** have magnetic moments of 2.26 and 1.77 BM at 2 K, which is below the limiting moment. Considering the antiferromagnetic interaction between terminal and central spin centers ($J = -46.64$ cm^{-1} and -47.27 cm^{-1} for **1** and **2**, respectively), the ground state should be a quartet state ($S = 3/2$). The theoretical value of μ_{eff} would be expected to be 3.87 BM at low temperatures. However, the relatively strong intermolecular interactions in **1** and **2** ($\theta = zJS(S + 1)/3k = -14.28$ K and -9.13 K) should also be taken into account. Thus, the μ_{eff} values of **1** and **2** decrease significantly at low temperatures.

Such a spin-state structure for compounds **1** and **2** is similar to those in the heterotrinuclear $Ni^{II}Cu^{II}Ni^{II}$ species reported by Kahn [22] and Liao [23]. For example, in Kahn's complex, {[Ni(bapa)(H₂O)]₂Cu(pba)}(ClO₄)₂ where bapa = bis(3-aminopropyl) and pba = 1,3-propyl-enebis(oxamato), the two high local spins exhibit an anti-ferromagnetic interaction with the small local spin and the small central spin polarizing the two high terminal spins in a ferromagnetic-like fashion.

Based on the structural analysis, there are no Ni–Ni bonds in **3** and **4**. The inner Ni^{2+} ions lie in a square planar coordination, and are therefore diamagnetic. The terminal Ni^{2+} ions are in a high-spin state and in a square pyramidal geometry, and have two unpaired electrons each. Fig. 7 shows the molar magnetic susceptibility and effective magnetic moments with respect to absolute temperature (K) for **4**. At 300 K the effective magnetic moment of 4.08 μ$_B$ is close to the expected value of 4.00 μ$_B$ for two non-interacting $S = 1$ spin states. When the temperature is lowered the value steadily decreases and reaches 2.52 μ$_B$ at 2 K. This behavior is indicative of two antiferromagnetically coupled high-spin Ni^{2+} ions in the terminal positions of the Ni_6^{12+} chain. Therefore, Eq. (4) can be used to fit the data for **3** and **4**:

$$\chi_M = \frac{Ng^2\beta^2}{k(T-\theta)} \times \frac{2e^{2J/kT} + 10e^{6J/kT}}{1 + 3e^{2J/kT} + 5e^{6J/kT}} \times (1-\rho)$$
$$+ \frac{2Ng^2\beta^2}{3kT} \times \rho + \chi_{TIP} \qquad (4)$$

This equation is based on an isotropic interaction between two $S = 1$ centers with the spin Hamiltonian, $H = -2J\widehat{S}_1 \cdot \widehat{S}_6$, and taking into account paramagnetic $S = 1$ impurities. The symbol J is the coupling constant between two terminal Ni^{2+} ions and the other symbols have been defined above. Both Ni_6^{12+} complexes reveal weak antiferromagnetic coupling of ca. $-5\,cm^{-1}$ between two terminal Ni^{2+} ions, consistent with our previous reports on multinuclear nickel complexes [14].

2.4. Electrochemical measurements

The electrochemical properties of **1** and **2** were investigated by cyclic voltammetry in CH_2Cl_2 solution with 0.1 M TBAP as the supporting electrolyte at a scan rate of 100 mV s^{-1}. The cyclic voltammograms exhibit three reversible redox waves at $E_{1/2}^{(1)} = +0.87$, $E_{1/2}^{(2)} = -0.02$ and $E_{1/2}^{(3)} = -0.46$ V for **1**, and $E_{1/2}^{(1)} = +0.96$, $E_{1/2}^{(2)} = -0.01$ and $E_{1/2}^{(3)} = -0.41$ V for **2**, where $E_{1/2}^{(1)}$, $E_{1/2}^{(2)}$ and $E_{1/2}^{(3)}$ correspond to Ni_6^{13+}/Ni_6^{12+}, Ni_6^{12+}/Ni_6^{11+} and Ni_6^{11+}/Ni_6^{10+}, respectively (Table 3). As an example, Fig. 8 shows the cyclic voltammogram of **1**. All of these electrochemical reactions involve one-electron processes, as judged by thin-layer spectroelectrochemical techniques. The oxidation observed at $E_{1/2}^{(2)} = -0.02$ can be assigned to one-electron abstraction from Ni_6^{11+} to generate the corresponding Ni_6^{12+} species. By comparison with the reported values of the analogous complexes [Ni₆(μ₆-bpyany)₄X₂](PF₆)₂ [19], the redox waves of **1** and **2** at $E_{1/2}^{(2)}$ and $E_{1/2}^{(3)}$ are anodically shifted in the range 210–270 mV. The significant difference in the redox potentials can be explained by the electron-withdrawing nature of the pyrimidyl groups of the supporting ligands. The smaller $E_{1/2}^{(2)}$ values for complexes **1** and **2** reflects their good stability under air. Thus, substitution of pyridyl with pyrimidyl groups allows us to fine-tune the redox properties of the complexes.

Spectroelectrochemistry was also conducted to confirm the oxidation states at a certain potential for **1** and **2**. Fig. 9 illustrates the absorption spectral changes of **2** at various applied potentials from -0.10 to $+0.20$ V in CH_2Cl_2 containing 0.1 M TBAP. As the applied potential

Table 3
Half-wave potentials of the redox couples

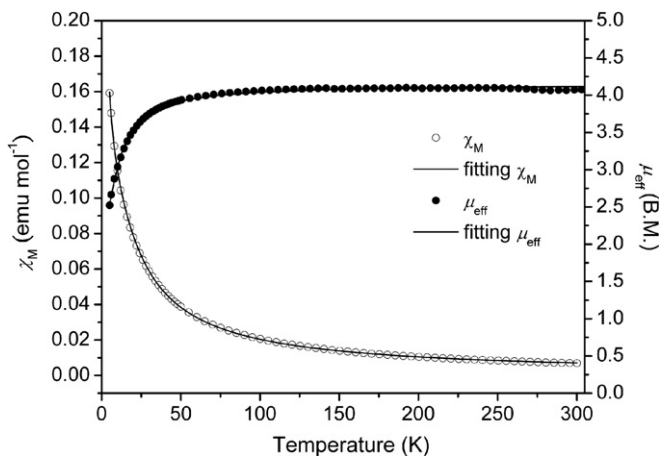|	$E_{1/2}^{(1)}$ (V)	$E_{1/2}^{(2)}$ (V)	$E_{1/2}^{(3)}$ (V)	
[Ni₆(μ₆-bpmany)₄Cl₂]⁺ (**1**)	+0.87	−0.02	−0.46	this work
[Ni₆(μ₆-bpmany)₄(NCS)₂]⁺ (**2**)	+0.96	−0.01	−0.41	this work
[Ni₆(μ₆-bpyany)₄Cl₂]⁺	+1.12	−0.23	−0.73	Ref. [19]
[Ni₆(μ₆-bpyany)₄(NCS)₂]⁺	+1.08	−0.22	−0.70	Ref. [19]

Fig. 7. The magnetic behavior for **4**: molar magnetic susceptibility χ$_M$ (○) and effective magnetic moments μ$_{eff}$ (●). The solid lines are the best-fit curves.
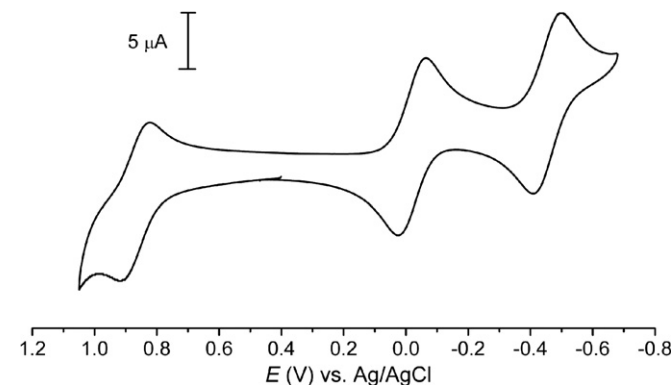

Fig. 8. The cyclic voltammograms of **1** in CH_2Cl_2 containing 0.1 M TBAP with a scan rate of 100 mV s^{-1}.
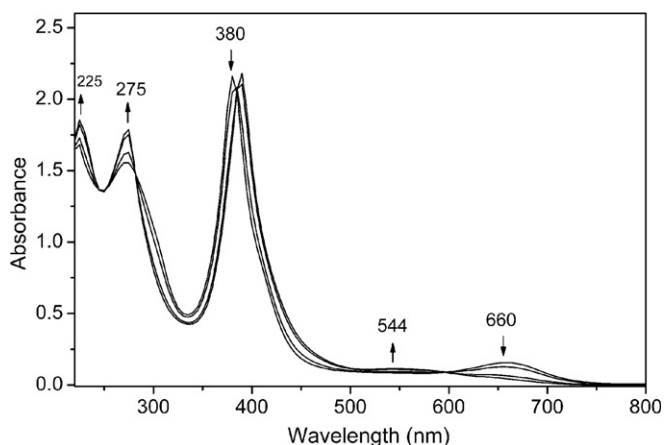
Fig. 9. Electronic absorption spectral changes for the first oxidation of **2** in CH_2Cl_2 containing 0.1 M TBAP at various applied potentials from −0.10 to +0.20 V.

increases, the peaks at 380 and 660 nm decrease in their absorption intensity whereas those at 225, 275, 390 and 544 nm increase with clear isosbestic points. The resulting spectrum is identical with that of complex **4** obtained by chemical methods.

3. Conclusions

The novel linear hexanickel string complexes **1**–**4** have been synthesized, and their magnetic and electrochemical properties have been investigated. Complexes **1**, **2** and **4** were structurally characterized. In the structures, the linear Ni_6 chain is helically wrapped by four all-*syn* type bpmany^{2-} ligands. The two terminal Ni^{2+} ions in all the complexes are in a high-spin state ($S = 1$). While complexes **3** and **4** (Ni_6^{12+}) do not show metal–metal bonding for the adjacent Ni^{2+} ions, the reduced forms **1** and **2** (Ni_6^{11+}) exhibit short Ni–Ni distances for the Ni_2 unit coordinated to the 1,8-naphthyridyl groups, indicating the presence of metal–metal interactions. The magnetic susceptibility and X-band EPR spectra agree well with the electronic structures in that one unpaired electron is located at the central Ni_2 unit for complexes **1** and **2**. These $Ni_6^{11+/12+}$ complexes may be used as molecular switches, since their electronic structure changes drastically upon oxidation or reduction. The STM (scanning tunneling microscopy) studies of complexes **2** and **4**, and the preparation of compounds containing $[M_6(bpmany)_4]^{n+}$ cores with other metal atoms or heterometal string complexes are underway in our laboratory.

4. Experimental

4.1. Materials

All Reagents were obtained from commercial suppliers and were used without further purification unless otherwise noted. The compounds 2-aminopyrimidine, naphthalene,

t-BuONa and NaSCN were purchased from Acros. Ferrocenium tetrafluoroborate and tetra-*n*-butylammonium perchlortae (TBAP) were purchased from Aldrich. Nickel acetate tetrahydrate, sodium tetrafloroborate, 1,3-bis(diphenylphosphino)propane (dppp) and $Pd_2(dba)_3$ were from Strem Chemicals. 2,7-Dichloro-1,8-naphthyridine was prepared according to literature procedures and modifications thereof [24].

4.2. Physical measurements

^{1}H NMR measurements were performed with a Varian 400 spectrometer with SiMe$_4$ as the internal reference. Magnetic susceptibility measurements on polycrystalline samples were carried out with a Quantum Design MPMS-7 SQUID magnetometer in the range of 2–300 K and using an applied field of 2000 G. Experimental data were corrected for the diamagnetic contribution calculated from Pascal's constants. Frozen solution X-band EPR spectra were recorded using a Bruker EMX-10 spectrometer. Electronic absorption spectra were measured in CH_2Cl_2 with a Hitachi U-3010 spectrophotometer. Infrared spectra were recorded on a Nicolet Magan 550 FT-IR spectrophotometer using KBr pellets. Elemental analyses were performed on a Perkin–Elmer CHN 2400. FAB mass spectra were obtained with a Hewlett–Packard 5890A spectrophotometer operating in the positive ion detection mode. Electrochemistry was carried out on a CHI 750A potentiostat in CH_2Cl_2 with 0.1 M TBAP. The cyclic voltammograms were recorded with a home-made three-electrode cell equipped with a BAS glassy carbon (0.07 cm^2) disk as the working electrode, a platinum wire as the auxiliary electrode and a home-made Ag/AgCl (saturated) reference electrode. The reference electrode was separated from the bulk solution by a double junction filled with electrolyte solution. Potentials are reported vs. Ag/AgCl (saturated) and referenced to the ferrocene–ferrocenium ([Cp$_2$Fe]/[Cp$_2$Fe]$^+$) couple which occurs at $E_{1/2}$ = +0.54 V vs. Ag/AgCl (saturated). The working electrode was polished with 0.03 μm aluminium on Buehler felt pads and was subjected to ultrasound for 1 min prior to each experiment. The reproducibility of individual potential values was within ±5 mV. Optical thin layer electrochemical (OTTLE) spectra were accomplished with the use of a 1 mm cuvette, a 100 mesh platinum gauze as the working electrode, a platinum wire as the auxiliary electrode and a Ag/AgCl (saturated) reference electrode.

4.3. Synthesis

4.3.1. 2,7-Bis(α-pyrimidylamino)-1,8-naphthyridine (H₂bpmany)

H$_2$bpmany was synthesized following the reported procedure using palladium catalyst [25]. To a mixture of 2-aminopyrimidine (4.18 g, 44 mmol), 2,7-dichloro-1,8-naphthyridine (3.98 g, 20 mmol) and *t*-BuONa (4.22 g, 44 mmol) in toluene (250 mL) were added Pd$_2$(dba)$_3$

(549 mg, 0.6 mmol) and 1,3-bis(diphenylphosphino)propane (dppp, 495 mg, 1.2 mmol). This mixture was stirred at 160 °C under an argon atmosphere for 2 d. After cooling to room temperature, the mixture was filtered, and then washed with toluene (3×50 mL), H_2O (3×100 mL) and MeOH (3×50 mL). The product was obtained as pale yellow solid, which was dried under vacuum (5.62 g, 89%). ^{1}H NMR (400 MHz, d_6-DMSO, 298 K, TMS): δ 10.24 (s, 2H; N*H*), 8.61 (d, $J = 4.8$ Hz, 4H; Pym*H*), 8.38 (d, $J = 8.8$ Hz, 2H; 4,5-Napy*H*), 8.21 (d, $J = 8.8$ Hz, 2H; 3,6-Napy*H*), 7.03 (t, $J = 4.8$ Hz, 2H; Pym*H*); IR (KBr): 3067, 3229, 3415 cm^{-1} (NH); ESI-MS: *m/z* (%): 317.31 (100) [M+H]$^+$; Elemental *Anal.* Calc. for $C_{16}H_{12}N_8$: C, 60.75; H, 3.82; N, 35.42. Found: C, 60.84; H, 3.72; N, 35.28%.

4.3.2. *[Ni$_6$(μ$_6$-bpmany)$_4$Cl$_2$]Cl (1)*

A 125 mL Erlenmeyer flask was charged with H_2bpmany (316 mg, 1 mmol), Ni(OAc)$_2 \cdot 4$ H_2O (373 mg, 1.5 mmol) and naphthalene (20 g). The mixture was heated at 200–210 °C for 3 h, and then excess LiCl (84 mg, 2 mmol) was carefully added, during which time the mixture became dark green. After the mixture was cooled to about 60 °C, *n*-hexane (3×100 mL) was used to remove naphthalene. The dry solid was extracted with CH_2Cl_2 and crystallized from CH_2Cl_2 and Et$_2$O to give dark green crystals (173 mg, 40%). UV/Vis (CH_2Cl_2): λ_{max} (ε) 232 (115,700), 278 (130,500), 382 (161,700), 656 nm (8500); FAB-MS: *m/z* (%): 1680.1 (40) [M]$^+$, 1644.9 (10) [M−Cl]$^+$, 1176.1 (100); Elemental *Anal.* Calc. for $C_{64}H_{40}Cl_3N_{32}Ni_6$: C, 44.80; H, 2.35; N, 26.12. Found: C, 44.54; H, 2.22; N, 26.28%.

4.3.3. *[Ni$_6$(μ$_6$-bpmany)$_4$(NCS)$_2$]Cl (2)*

Complex **2** was synthesized using a procedure similar to that for **1** except that NaSCN (162 mg, 2 mmol) was used instead of LiCl. Dark green crystals were obtained by slow diffusion of Et$_2$O into the solution of product in CH_2Cl_2 and CH_3CN (124 mg, 28%). IR (KBr): 2067 cm^{-1} (C≡N); UV/Vis (CH_2Cl_2): λ_{max} (ε) 232 (136,800), 274 (137,800), 384 (172,400), 654 nm (9300); FAB-MS: *m/z* (%): 1724.4 (25) [M]$^+$, 1667.4 (20) [M−NCS]$^+$, 1176.5 (100); Elemental *Anal.* Calc. (%) for $C_{66}H_{40}ClN_{34}Ni_6S_2$: C, 45.01; H, 2.29; N, 27.04. Found: C, 44.74; H, 2.42; N, 26.49%.

4.3.4. *[Ni$_6$(μ$_6$-bpmany)$_4$Cl$_2$](BF$_4$)$_2$ (3)*

A 50 mL round-bottomed flask containing **1** (86 mg, 0.05 mmol) and ferrocenium tetrafluoroborate (14 mg, 0.05 mmol) was charged with CH_2Cl_2 (20 mL) at room temperature. The initially dark green solution became dark brown upon stirring. The solution was stirred for 1 h, and then Et$_2$O were added to precipitate a dark brown solid. The solid was extracted with CH_2Cl_2 and crystallized from MeCN and Et$_2$O to give dark brown crystals (26 mg, 28%). UV/Vis (CH_2Cl_2): λ_{max} (ε) 230 (124,700), 274 (136,400), 388 (164,300); FAB-MS: *m/z* (%): 1680.0 (50) [M]$^+$, 1645.0 (10) [M−Cl]$^+$, 1176.1 (100); Elemental *Anal.* Calc.

for $C_{64}H_{40}B_2Cl_2F_8N_{32}Ni_6$: C, 41.46; H, 2.17; N, 24.18. Found: C, 42.04; H, 2.43; N, 24.71%.

4.3.5. *[Ni$_6$(μ$_6$-bpmany)$_4$(NCS)$_2$](BF$_4$)$_2$ (4)*

A procedure similar to that for complex **3** was employed. Dark brown crystals were obtained by slow diffusion of Et$_2$O into the solution of the product in CH_3CN (32 mg, 34%). IR (KBr): 2067 cm^{-1} (C≡N); UV/Vis (CH_2Cl_2): λ_{max} (ε) 232 (117,300), 274 (131,600), 388 (166,100); FAB-MS: *m/z* (%): 1723.9 (25) [M]$^+$, 1666.9 (15) [M−NCS]$^+$, 1176.0 (100); Elemental *Anal.* Calc. for $C_{66}H_{40}B_2F_8N_{34}Ni_6S_2$: C, 41.74; H, 2.12; N, 25.08. Found: C, 42.10; H, 2.41; N, 25.43%.

4.4. X-ray crystallographic determinations

Crystallographic information for **1**, **2** and **4** are summarized in Table 1. The chosen crystals were mounted on a glass fiber. X-ray diffraction data for **1**, **2** and **4** were collected at 150 K on a NONIUS Kappa CCD diffractometer installed with monochromatized Mo Kα radiation, $\lambda = 0.71073$ Å. Cell parameters were retrieved and refined using DENZO-SMN software on all observed reflections [26]. Data reduction was performed with the DENZO-SMN software [27]. An empirical absorption was based on the symmetry-equivalent reflections and absorption corrections were applied with the SORTAV program. All the structures were solved by using SHELXS-97 [28] and refined with SHELXL-97 [29] by full-matrix least squares on F^2 values. Hydrogen atoms were fixed at calculated positions and refined using a riding model.

Appendix A. Supplementary material

CCDC 626037, 626038 and 626039 contain the supplementary crystallographic data for **1**, **2** and **4**. These data can be obtained free of charge via http://www.ccdc.cam.ac.uk/conts/retrieving.html, or from the Cambridge Crystallographic Data Centre, 12 Union Road, Cambridge CB2 1EZ, UK; fax: (+44) 1223-336-033; or e-mail: deposit@ccdc.cam.ac.uk. Supplementary data associated with this article can be found, in the online version, at doi:10.1016/j.poly.2007.04.036.

References

[1] (a) L.-P. Wu, P. Field, T. Morrissey, C. Murphy, P. Nagle, B. Hathaway, C. Simmons, P. Thornton, J. Chem. Soc., Dalton Trans. (1990) 3835;
(b) G.J. Pyrka, M. El-Mekki, A.A. Pinkerton, J. Chem. Soc., Chem. Commun. (1991) 84.
[2] S. Aduldecha, B. Hathaway, J. Chem. Soc., Dalton Trans. (1991) 993.

[3] (a) F.A. Cotton, L.M. Daniels, C.A. Murillo, I. Pascual, J. Am. Chem. Soc. 119 (1997) 10223;
(b) R. Clérac, F.A. Cotton, L.M. Daniels, K.R. Dunbar, C.A. Murillo, I. Pascual, Inorg. Chem. 39 (2000) 748;
(c) R. Clérac, F.A. Cotton, L.M. Daniels, K.R. Dunbar, C.A. Murillo, I. Pascual, Inorg. Chem. 39 (2000) 752;
(d) F.A. Cotton, L.M. Daniels, P. Lei, C.A. Murillo, X. Wang, Inorg. Chem. 40 (2001) 2778;
(e) J.F. Berry, F.A. Cotton, C.A. Murillo, B.K. Roberts, Inorg. Chem. 43 (2004) 2277.

[4] (a) F.A. Cotton, L.M. Daniels, G.T. Jordan IV, C.A. Murillo, J. Am. Chem. Soc. 119 (1997) 10377;
(b) M. Rohmer, M. Bénard, J. Am. Chem. Soc. 120 (1998) 9372;
(c) F.A. Cotton, C.A. Murillo, X. Wang, J. Chem. Soc., Dalton Trans. (1999) 3327;
(d) F.A. Cotton, C.A. Murillo, X. Wang, Inorg. Chem. 38 (1999) 6294;
(e) R. Clérac, F.A. Cotton, K.R. Dunbar, T. Lu, C.A. Murillo, X. Wang, Inorg. Chem. 39 (2000) 3065;
(f) R. Clérac, F.A. Cotton, K.R. Dunbar, T. Lu, C.A. Murillo, X. Wang, J. Am. Chem. Soc. 122 (2000) 2272;
(g) R. Clérac, F.A. Cotton, L.M. Daniels, K.R. Dunbar, K. Kirschbaum, C.A. Murillo, A.A. Pinkerton, A.J. Schultz, X. Wang, J. Am. Chem. Soc. 122 (2000) 6226;
(h) R. Clérac, F.A. Cotton, L.M. Daniels, K.R. Dunbar, C.A. Murillo, X. Wang, Inorg. Chem. 40 (2001) 1256;
(i) R. Clérac, F.A. Cotton, S.P. Jeffery, C.A. Murillo, X. Wang, Inorg. Chem. 40 (2001) 1265.

[5] (a) R. Clérac, F.A. Cotton, K.R. Dunbar, C.A. Murillo, I. Pascual, X. Wang, Inorg. Chem. 38 (1999) 2655;
(b) J.F. Berry, F.A. Cotton, L.M. Daniels, C.A. Murillo, J. Am. Chem. Soc. 124 (2002) 3212;
(c) J.F. Berry, F.A. Cotton, C.A. Murillo, J. Chem. Soc., Dalton Trans. (2003) 3015;
(d) J.F. Berry, F.A. Cotton, L.M. Daniels, C.A. Murillo, X. Wang, Inorg. Chem. 42 (2003) 2418.

[6] J.F. Berry, F.A. Cotton, P. Lei, C.A. Murillo, Inorg. Chem. 42 (2003) 377.

[7] (a) J.-T. Sheu, C.-C. Lin, I. Chao, C.-C. Wang, S.-M. Peng, Chem. Commun. (1996) 315;
(b) C.-K. Kuo, J.-C. Chang, C.-Y. Yeh, G.-H. Lee, C.-C. Wang, S.-M. Peng, J. Chem. Soc., Dalton Trans. (2005) 3696.

[8] S.-Y. Lai, T.-W. Lin, Y.-H. Chen, C.-C. Wang, G.-H. Lee, M.-H. Yang, M.-K. Leung, S.-M. Peng, J. Am. Chem. Soc. 21 (1999) 250.

[9] (a) F.A. Cotton, L.M. Daniels, T. Lu, C.A. Murillo, X. Wang, Chem. Commun. (1999) 2461;
(b) F.A. Cotton, L.M. Daniels, T. Lu, C.A. Murillo, X. Wang, J. Chem. Soc., Dalton Trans. (1999) 517;
(c) H.-C. Chang, J.-T. Li, C.-C. Wang, T.-W. Lin, H.-C. Lee, G.-H. Lee, S.-M. Peng, Eur. J. Inorg. Chem. (1999) 1243.

[10] (a) S.-J. Shieh, C.-C. Chou, G.-H. Lee, C.-C. Wang, S.-M. Peng, Angew. Chem., Int. Ed. Engl. 36 (1997) 56;
(b) C.-Y. Yeh, C.-H. Chou, K.-C. Pan, C.-C. Wang, G.-H. Lee, Y.O. Su, S.-M. Peng, J. Chem. Soc., Dalton Trans. (2002) 2670.

[11] (a) C.-C. Wang, W.-C. Lo, C.-C. Chou, G.-H. Lee, J.-M. Chen, S.-M. Peng, Inorg. Chem. 37 (1998) 4059;
(b) C.-Y. Yeh, Y.-L. Chiang, G.-H. Lee, S.-M. Peng, Inorg. Chem. 41 (2002) 4096.

[12] Y.-H. Chen, C.-C. Lee, C.-C. Wang, S.-Y. Lai, F.-Y. Li, C.-Y. Mou, S.-M. Peng, Chem. Commun. (1999) 1667.

[13] S.-Y. Lai, C.-C. Wang, Y.-H. Chen, C.-C. Lee, Y.-H. Liu, S.-M. Peng, J. Chin. Chem. Soc. 46 (1999) 477.

[14] S.-M. Peng, C.-C. Wang, Y.-L. Jang, Y.-H. Chen, F.-Y. Li, C.-Y. Mou, M.-K. Leung, J. Magn. Magn. Mater. 209 (2000) 80.

[15] (a) A. Clearfield, P. Singh, I. Bernal, J. Chem. Soc., Chem. Commun. (1970) 389;
(b) P. Singh, A. Clearfield, I. Bernal, J. Coord. Chem. 1 (1971) 29;
(c) A. Døssing, S. Larsen, A.V. Lelieveld, R.M. Bruun, Acta Chem. Scand. 53 (1999) 230.

[16] (a) D. Gatteschi, C. Mealli, L. Sacconi, J. Am. Chem. Soc. 95 (1973) 2736;
(b) L. Sacconi, C. Mealli, D. Gatteschi, Inorg. Chem. 13 (1974) 1985;
(c) A. Bencini, D. Gatteschi, L. Sacconi, Inorg. Chem. 17 (1978) 2670;
(d) A. Bencini, E. Berti, A. Caneschi, D. Gatteschi, E. Giannasi, I. Invernizzi, Chem. Eur. J. 8 (2002) 3660.

[17] (a) W.R. Tikkanen, E. Binamira-Soriaga, W.C. Kaska, P.C. Ford, Inorg. Chem. 22 (1983) 1147;
(b) W.R. Tikkanen, E. Binamira-Soriaga, W.C. Kaska, P.C. Ford, Inorg. Chem. 23 (1984) 141;
(c) W.R. Tikkanen, C. Krüger, K.D. Bomben, W.L. Jolly, W.C. Kaska, P.C. Ford, Inorg. Chem. 23 (1984) 3633;
(d) E. Binamira-Soriaga, N.L. Keder, W.C. Kaska, Inorg. Chem. 29 (1990) 3167.

[18] C.-H. Chien, J.-C. Chang, C.-Y. Yeh, G.-H. Lee, J.-M. Fang, S.-M. Peng, J. Chem. Soc., Dalton Trans. (2006) 2106.

[19] C.-H. Chien, J.-C. Chang, C.-Y. Yeh, G.-H. Lee, J.-M. Fang, Y. Song, S.-M. Peng, J. Chem. Soc., Dalton Trans. (2006) 3249.

[20] T.S. Calderwood, T.C. Bruice, Inorg. Chem. 25 (1986) 3722.

[21] O. Kahn, Molecular Magnetism, Wiley-VCH, New York, 1993.

[22] (a) Y. Pei, Y. Journaux, O. Kahn, Inorg. Chem. 27 (1988) 399;
(b) J. Ribas, C. Diaz, R. Costa, Y. Journaux, C. Mathoniere, O. Kahn, A. Gleizes, Inorg. Chem. 29 (1990) 2042.

[23] (a) E.-Q. Gao, J.-K. Tang, D.-Z. Liao, Z.-H. Jiang, S.-P. Yan, G.-L. Wang, Inorg. Chem. 40 (2001) 3134;
(b) Q.-L. Wang, L.-N. Zhu, D.-Z. Liao, S.-P. Yan, Z.-H. Jiang, P. Cheng, G.-M. Yang, J. Mol. Struct. 754 (2005) 10.

[24] G.R. Newkome, S.J. Garbis, V.K. Majestic, F.R. Fronczek, G. Chiari, J. Org. Chem. 46 (1981) 833.

[25] S. Wagaw, S.L. Buchwald, J. Org. Chem. 61 (1996) 7240.

[26] Z. Otwinowski, W. Minor, Methods Enzymol. 276 (1997) 307.

[27] R.H. Blessing, Acta. Crystallogr., Sect. A 51 (1995) 33.

[28] G.M. Sheldrick, Acta. Crystallogr., Sect. A 46 (1990) 467.

[29] G.M. Sheldrick, SHELXL-97, University of Göttingen, Germany, 1997.